Letter

Magnetic tuning of the tunnel coupling in an optically active quantum dot molecule

Frederik Bopp,[1,*] Charlotte Cullip,[1,*] Christopher Thalacker,[1] Michelle Lienhart,[1] Johannes Schall,[2] Nikolai Bart,[3] Friedrich Sbresny,[4] Katarina Boos,[4] Sven Rodt,[2] Dirk Reuter,[5] Arne Ludwig,[3] Andreas D. Wieck,[3] Stephan Reitzenstein,[2] Filippo Troiani,[6] Guido Goldoni,[6,7] Elisa Molinari,[6,7] Kai Müller,[4] and Jonathan J. Finley[1,†]

[1]*Walter Schottky Institut, School of Natural Sciences, and MCQST, Technische Universität München, Am Coulombwall 4, 85748 Garching, Germany*

[2]*Institut für Festkörperphysik, Technische Universität Berlin, Hardenbergstraße 36, 10623 Berlin, Germany*

[3]*Lehrstuhl für Angewandte Festkörperphysik, Ruhr-Universität Bochum, Universitätsstraße 150, 44801 Bochum, Germany*

[4]*Walter Schottky Institut, School of Computation, Information and Technology, and MCQST, Technische Universität München, Am Coulombwall 4, 85748 Garching, Germany*

[5]*Paderborn University, Department of Physics, Warburger Straße 100, 33098 Paderborn, Germany*

[6]*Centro S3, CNR-Istituto Nanoscienze, Via Campi 213/a, 41125 Modena, Italy*

[7]*Dipartimento di Scienze Fisiche, Informatiche e Matematiche, Università di Modena e Reggio Emilia, Via Campi 213/a, 41125 Modena, Italy*

(Received 22 March 2023; revised 6 February 2025; accepted 7 July 2025; published 8 August 2025)

Self-assembled optically active quantum dot molecules (QDMs) allow the creation of protected qubits via singlet-triplet spin states. The qubit energy splitting of these states is defined by the tunnel coupling strength and is, therefore, determined by the potential landscape and is fixed during growth. Applying an in-plane magnetic field increases the confinement of the hybridized wave functions within the quantum dots, leading to a decrease of the tunnel coupling strength. We achieve a tuning of the coupling strength by 53.4% ± 1.7%. The ability to fine-tune this coupling is essential for quantum network and computing applications that require quantum systems with near identical performance.

DOI: 10.1103/dhjc-fvh3

Although any physical qubit is susceptible to dephasing, the use of protected qubits offers a way to passively shield the quantum information from their noise environment [1,2]. Few-spin solid-state qubits are particularly promising in this regard, since they are immune to the dominant electric and magnetic field noise sources to first order [3–5]. Recently, the extension of the spin coherence time by creating a few-spin (e.g., singlet-triplet) qubit has been demonstrated in a vertically stacked pair of optically active quantum dots [6]. Such quantum dot molecules (QDMs) combine the advantages of single quantum dots (QDs), such as robust optical selection rules [7] and dominant emission into the zero-phonon line [8], with the ability to create protected few-spin qubits [5]. They are formed from two vertically stacked QDs separated by a tunnel barrier. At a separation of a few nanometers, the orbital states in the two dots become tunnel coupled with a strength that depends on the separation of the dots and the height of the tunnel barrier [9]. Tunnel coupling facilitates the creation of hybridized symmetric and antisymmetric few-spin states, which serve as protected qubit eigenstates [10]. The energy splitting between these two states is defined by the tunnel coupling. This makes the coupling strength the main tuning parameter of the solid-state qubit, as it determines the operating rate of quantum gates [11]. However, the thickness and height of the tunnel barrier are fixed during the growth process. By establishing a method for post-growth continuous and reversible tuning of the tunnel coupling, synchronization of multiple qubits could be enabled to facilitate applications such as quantum networks [12]. In addition, the generation of two-dimensional photonic cluster states for measurement-based quantum computing could be optimized [13,14].

One approach to control the tunnel coupling post-growth is to apply strain to the system. However, so far only weak energy shifts up to 50 μeV have been achieved experimentally [15] while lacking long-term stability [16]. A second approach to tune the tunnel coupling, promising a wider tuning range with higher temporal stability, is to apply a static magnetic field to the QDM. This results in a modification of the orbital part of the carrier wave function and, therefore, control of the tunnel coupling. Over the past decades, several theoretical works have explored the magnetic tuning of symmetric and antisymmetric orbitals in artificial molecules [17–22]. However, experimental demonstrations have not yet been provided [23,24] and structure-property relationships are yet to be established. In-plane magnetic fields are predicted to result in a confinement of the orbital part of the wave function along a direction perpendicular to the field direction (diamagnetic response), corresponding to a reduction of the tunnel coupling [19]. To qualitatively illustrate the magnetic field dependence of the wave function, Fig. 1(a) shows a sketch of the electron wave function in a double-well potential without (solid) and

*These authors contributed equally to this work.
†finley@wsi.tum.de

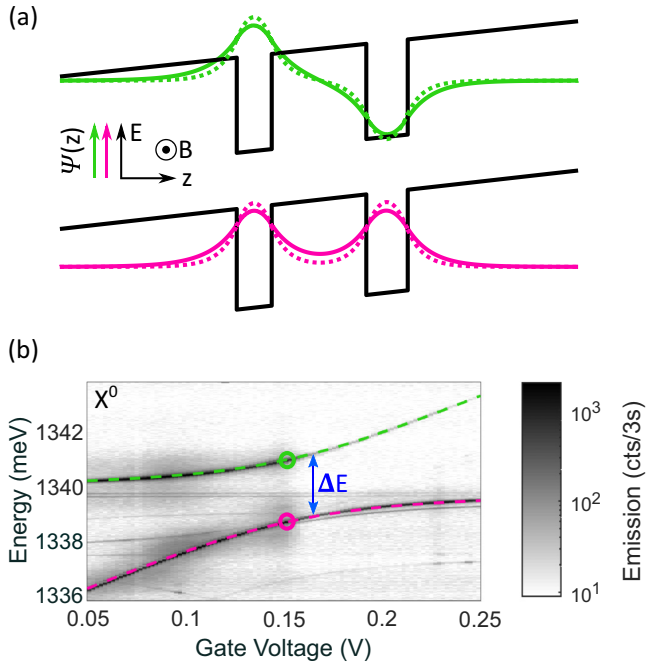

FIG. 1. Tunnel coupling of the neutral exciton (X^0). (a) Schematic of bonding (pink) and antibonding (green) wave function $\Psi(z)$ of the lowest and second lowest electron energy eigenstate, respectively, with (dashed) and without (solid) applied in-plane magnetic field B. The solid black lines depict the electron trapping potential along the growth direction z. (b) Voltage-dependent photoluminescence measurement of the X^0. The energy splitting between the bonding (pink) and antibonding (green) eigenstates ΔE is depicted by a blue arrow, while the energy of the tunnel-coupled states is visualized by colored circles.

with (dashed) magnetic field B applied along the x direction. The pink (green) wave function $\Psi(z)$ illustrates the lowest symmetric (second lowest, antisymmetric) eigenstate of a single electron confined in the QDM potential. The solid black lines represent an approximate potential landscape of the QDM along the growth direction z. The probability density of the charge position inside the two potential wells is predicted to increase at higher magnetic fields because of magnetic compression of the wave function [19]. Consequently, the wave function is expelled from the barrier region between the two potentials wells, which effectively reduces the strength of the tunnel coupling.

In this work, we experimentally demonstrate the tunability of the tunnel coupling of an artificial molecule by varying an in-plane magnetic field. We perform magneto-photoluminescence measurements on a single QDM to study the energy splitting between the bonding (BO) and antibonding (AB) neutral exciton (X^0) states and hence the tunnel coupling strength. We observe a reduced splitting with increasing magnetic field, which we numerically simulate by modeling a three-dimensional confinement potential and calculating the corresponding single-particle energies and Coulomb interactions between the localized carriers. By applying an electric field along the growth direction, we tune the electronic levels of the two dots into and out of resonance. This allows us to conclusively show that the magnetic field leads to a reduction of the tunnel coupling strength, providing a post-growth control of this parameter.

The QDM investigated in this work consists of two vertically stacked and tunnel-coupled InAs QDs embedded in a GaAs matrix [25]. The neutral exciton (X^0) is used to demonstrate the general reduction of the energy gap between BO and AB eigenstates. Excitation of the neutral exciton is achieved via a continuous wave laser resonant to a higher orbital shell at 1353.6 meV, while the s-shell emission is monitored. To efficiently excite the X^0 state, a two-phase optical and electrical sequence is used for all measurements presented in this letter [26]. The applied gate voltage allows tuning of the energy levels of the two QDs relative to each other. In combination with the tunnel coupling, this allows the hybridization of charge wave functions forming BO and AB eigenstates. An avoided crossing is the result. Figure 1(b) shows the voltage-dependent photoluminescence of the X^0 state. The eigenenergies corresponding to the BO and AB eigenstates are highlighted by dashed pink and green fits, respectively. The exciton energies are fitted using a coupled two-state model, including a linear bias and a quadratic contribution proportional to the bias, which accounts for the DC Stark effect for indirect and direct excitons, respectively [27]. The full description can be found in the Supplemental Material [28] and Refs. [2,3] therein.

The voltage at which hybridization of the two wave functions occurs is depicted by the colored circles in Fig. 1(b). The minimum energy difference ΔE between the two exciton eigenstates is solely determined by the strength of the tunnel coupling t. Since we work in a regime where the electron can hybridize while the hole remains confined in the upper QD [9], the energy splitting between the BO and AB eigenstates ΔE corresponds to the energy difference between the observed neutral exciton eigenstates. This allows us to analyze the magnetic field-dependent energy separation between the BO and AB wave functions and thus obtain the tunnel coupling between the QDs.

To analyze the *in situ* tunability of the tunnel coupling, we apply an in-plane magnetic field along the x direction (Voigt geometry). Figure 2(a) shows a magneto-photoluminescence measurement of the BO and AB state at the lowest splitting of 0.15 V. In addition to a diamagnetic shift [29], the magnetic field leads to a mixing of bright and dark exciton states [30] and a Zeeman splitting of the spin states [31]. This results in the occurrence of the four allowed optical transitions for both the BO and AB eigenstates, as shown by the single photoluminescence trace in Fig. 2(a) recorded at 15 T. With an increasing magnetic field, the energy separation ΔE between the eigenstates with the same spin configuration reduces. We define ΔE as the difference between the highest energy transition of the BO and of the corresponding AB eigenstate.

Figure 2(b) shows the energy splitting ΔE as a function of magnetic field. The blue data points describe the energy separation at 0.15 V obtained from Fig. 2(a). The energy separation between the two eigenstates decreases with increasing magnetic field. In order to unambiguously identify the observed transitions, we complement the experimental results with numerical calculations, performed within the envelope function and the effective-mass approach [32]. The single-particle energies and eigenstates are obtained by diagonalizing on a real-space grid of 524 288 points, using a Hamiltonian

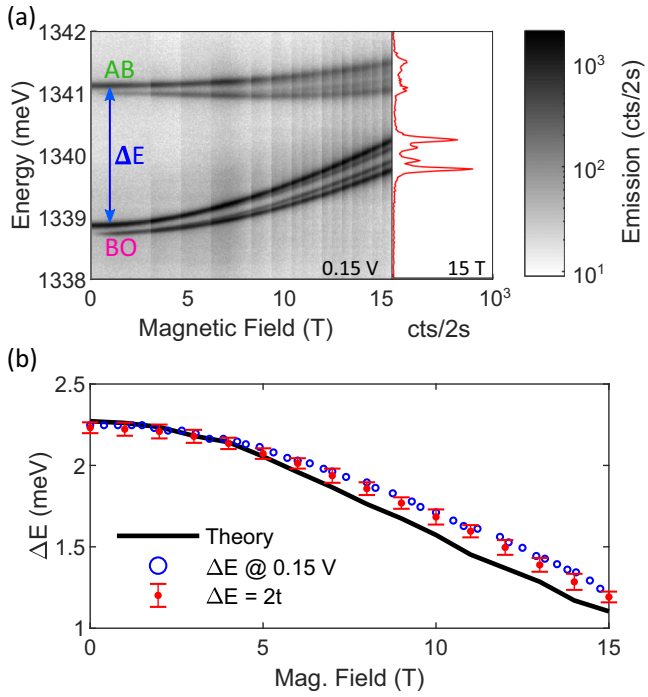

FIG. 2. (a) Magneto-photoluminescence measurement in the tunnel-coupling regime at 0.15 V. The energy splitting ΔE between the bonding (BO) and antibonding (AB) eigenstate is illustrated by a blue arrow. The red solid line shows the emission spectrum at 15 T. (b) The energy splitting ΔE as function of the magnetic field. The blue data points indicate the energy splitting between the highest-energy transitions of the BO and the AB eigenstate at 0.15 V. The red data points are extracted from fitting the voltage-dependent energy splitting. The black solid line shows the numerically predicted energy splitting ΔE.

that includes a kinetic and a potential contribution,

$$H_\chi(\mathbf{r}) = \frac{1}{2m^*_\chi}\left(-i\hbar\nabla + \frac{q_\chi}{c}\mathbf{A}\right)^2 + V_\chi(\mathbf{r}), \qquad (1)$$

where $\mathbf{A} = \frac{1}{2}\mathbf{B}\times\mathbf{r}$ is the vector potential, $\chi = e, h$ specifies the particle type and its charge ($q_h = -q_e = |e|$), and m^*_χ is the effective mass. The confinement potential includes a parabolic in-plane contribution, $V_{xy,\chi}(x,y) = \frac{1}{2}m^*_\chi\omega^2_\chi(x^2 + y^2)$, and a double square well in the vertical (z) direction. In particular, the two wells have widths of $d_1 = 2.7$ nm and $d_2 = 2.9$ nm, matching the height of the bottom and top single QD, respectively. We note that the dot heights were precisely fixed at these values using the In-flush method [33]. Similarly, the barrier between the two dots was defined during growth and fixed at $l = 7.3$ nm. The height of the barrier is set to $V_0 = 690$ meV, corresponding to the conduction band offset of strained InAs and GaAs [34]. In addition, the potential includes a linear term $V_{\text{bias},\chi} = q_\chi\mathcal{E}z$, with $\mathcal{E} = 3.63$ meV/nm to account for the electric field.

We include the Coulomb interaction perturbatively, and identify the energy of the lowest (first excited) exciton state with the sum of the electron ground state energy, the hole ground state energy, and the direct Coulomb matrix element involving these single-particle states. Further details are provided in the Supplemental Material [28].

The black solid curve in Fig. 2(b) shows the numerically obtained energy splitting ΔE as a function of the strength of the in-plane magnetic field. We obtain an excellent qualitative agreement between experimental and theoretical results. Quantitative differences may result from simplifications in the applied three-dimensional potential.

The magnetic field leads to an enhanced confinement of the charges in the potential wells along the growth direction z, which is associated with a reduction of the electron wave function density inside the tunneling barrier. Thus, the coupling strength decreases with increasing magnetic field. In the presented magnetic field range we observe a decrease of the splitting of the avoided crossing by $53.4\% \pm 1.7\%$, which corresponds to an absolute energy shift of (-1.04 ± 0.05) meV and a change of the tunnel coupling strength from $t = (1.12 \pm 0.02)$ meV to (0.60 ± 0.02) meV. Our previous theoretical study [19] demonstrated that the observed reduction arises from a general reduction of the amplitude of the wavefunction within the AlGaAs barrier, rather than a magnetic field dependent difference of the diamagnetic coefficient of the hybridized excitonic states. This finding was shown to be quite general, independent of the precise form of the confinement potential along the axis of the QD molecule. The observed magnetic reduction of the tunnel coupling is a factor of $21\times$ higher than what could be previously achieved by strain tuning the device [15].

As the magnetic field is increased, the decrease in ΔE, and hence the tunnel coupling, should be maximal in the center of the avoided crossing. Thus, we continue to analyze ΔE close to and away from the avoided crossing to show conclusively that the reduction of ΔE is indeed caused by a reduction of the tunnel coupling. Therefore, we measured ΔE for different DC gate voltages tracking over the avoided crossing.

Figure 3(a) shows ΔE as a function of the gate voltage around the avoided crossing at 0 T (black points) and 15 T (blue points). The solid lines result from fitting the data with the difference of the eigenenergies calculated from the coupled two-state model. Both fits show a minimum at the center voltage of the avoided crossing, depicted by the vertical dashed lines. V_C marks the center voltage of the avoided crossing at 0 T. As before, ΔE is reduced at 15 T compared to 0 T. This results in a reduced tunneling coupling strength, represented by the fit parameter t. At V_C the energy splitting is $\Delta E = 2t$, which allows the extraction of the minimum splitting from the applied fit. The red data points in Fig. 2(b) show the minimum energy splitting for different magnetic fields. While the fitted and measured ΔE are in excellent agreement at low magnetic fields, a small deviation is observed at higher fields. This is caused by a magnetic field-dependent shift of V_C. The inset in Fig. 3(a) shows the evolution of V_C with increasing magnetic field. The observed voltage shift of the tunnel coupling originates from the different sizes of the two individual QDs. By increasing the magnetic field and thus the confinement of the charge, the eigenenergies of the two QDs encounter different energy shifts. As a result, a lower gate voltage is required to attain the coupling condition. Thus, V_C decreases with increasing magnetic field.

To demonstrate the reduction in energy splitting at the avoided crossing, we analyze the difference of ΔE with and without an applied magnetic field. Figure 3(b) shows

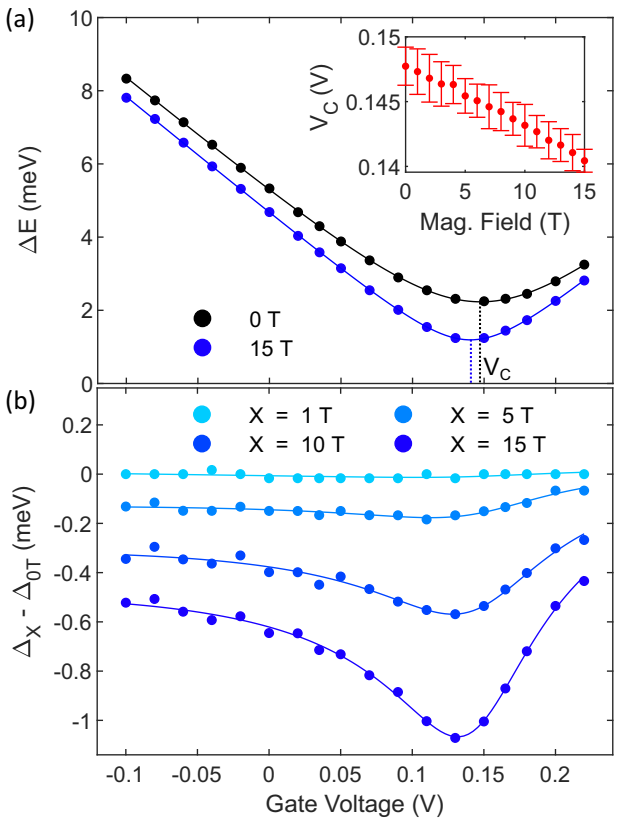

FIG. 3. (a) ΔE as a function of the gate voltage at 0 T (black dots) and 15 T (blue dots). Solid lines visualize the fit of the energy splitting. V_C describes the voltage, where ΔE is minimal. The inset shows V_C as function of the magnetic field. (b) Difference of ΔE with and without applied magnetic field as a function of the gate voltage. The solid lines show the difference between the fits applied in (a).

the voltage-dependent difference $\Delta_{X\,\mathrm{T}}$ - $\Delta_{0\,\mathrm{T}}$, with $X \in \{1, 5, 10, 15\}$. The fitted curves (solid lines) are obtained by subtracting the difference of the fitted eigenenergies in Fig. 3(a). The asymmetry of the curve is caused by the change in V_C with increasing magnetic field, as discussed before. The data presented exhibit a minimum of the energy difference at the avoided crossing. This minimum confirms that the variation of the energy splitting is indeed maximal at the avoided crossing. Thus, we can conclude that the applied magnetic field reduces the tunnel coupling between the two quantum dots.

In summary, we have demonstrated a reduction in the energy splitting between BO and AB eigenstates of a QDM by applying in-plane magnetic fields. This corresponds to a reduction in the tunnel coupling strength between the two QDs. Fitting the energy difference between the eigenstates of the system to the voltage and magnetic field-dependent measurements allows quantification of the variation of the tunnel coupling strength. We obtain a wide tuning range of $53.4\% \pm 1.7\%$ with a maximum tuning rate of $(-101 \pm 6)\,\mu\mathrm{eV/T}$. The decrease of the absolute energy splitting is (1.04 ± 0.05) meV. Our results confirm several theoretical predictions [17–22] and demonstrate that in-plane magnetic fields enable the tuning of the tunnel coupling in QDMs.

The tunability of the tunnel coupling is crucial for controlling the eigenstates of solid-state qubits in QDMs. The presented results allow optimization of the gate operations for the generation of two-dimensional photonic cluster states [13]. Moreover, tuning the eigenenergies of a qubit facilitates its synchronization with other qubits and thus their entanglement to enable multi-qubit networks. These results are generally applicable to other artificial molecules, e.g., in two-dimensional materials with a similar trapping potential [17].

The authors gratefully acknowledge financial support from the German Federal Ministry of Education and Research (BMBF) via Q.Link.X (16KIS0874, 16KIS0863, 16KIS086), QR.X (16KISQ027, 16KISQ014, 16KISQ012, and 16KISQ009), MOQUA (13N14846), the Horizon 2020 research and innovation program of the European Union under Grant Agreement No. 862035 (QLUSTER) and the Deutsche Forschungsgemeinschaft (DFG, German Research Foundation) via SQAM (FI947-5-1), DIP (FI947-6-1), and the Excellence Cluster MCQST (EXC-2111, 390814868). F.B. gratefully acknowledges the Exploring Quantum Matter (ExQM) programme funded by the State of Bavaria. F.T. and E.M. acknowledge financial support from the European Commission through the Project IQubits (Call H2020FETOPEN20182019202001, Project Id 829005).

[1] D. A. Lidar, I. L. Chuang, and K. B. Whaley, Decoherence-free subspaces for quantum computation, Phys. Rev. Lett. **81**, 2594 (1998).

[2] B. Douçot and L. B. Ioffe, Physical implementation of protected qubits, Rep. Prog. Phys. **75**, 072001 (2012).

[3] J. R. Petta, A. C. Johnson, J. M. Taylor, E. A. Laird, A. Yacoby, M. D. Lukin, C. M. Marcus, M. P. Hanson, and A. C. Gossard, Coherent manipulation of coupled electron spins in semiconductor quantum dots, Science **309**, 2180 (2005).

[4] M. Stopa and C. M. Marcus, Magnetic field control of exchange and noise immunity in double quantum dots, Nano Lett. **8**, 1778 (2008).

[5] K. M. Weiss, J. M. Elzerman, Y. L. Delley, J. Miguel-Sanchez, and A. Imamoğlu, Coherent two-electron spin qubits in an optically active pair of coupled InGaAs quantum dots, Phys. Rev. Lett. **109**, 107401 (2012).

[6] K. X. Tran, A. S. Bracker, M. K. Yakes, J. Q. Grim, and S. G. Carter, Enhanced spin coherence of a self-assembled quantum dot molecule at the optimal electrical bias, Phys. Rev. Lett. **129**, 027403 (2022).

[7] Y. Benny, S. Khatsevich, Y. Kodriano, E. Poem, R. Presman, D. Galushko, P. M. Petroff, and D. Gershoni, Coherent optical writing and reading of the exciton spin state in single quantum dots, Phys. Rev. Lett. **106**, 040504 (2011).

[8] I. Favero, G. Cassabois, R. Ferreira, D. Darson, C. Voisin, J. Tignon, C. Delalande, G. Bastard, Ph. Roussignol, and J. M. Gérard, Acoustic phonon sidebands in the emission line of single InAs/GaAs quantum dots, Phys. Rev. B **68**, 233301 (2003).

[9] A. S. Bracker, M. Scheibner, M. F. Doty, E. A. Stinaff, I. V. Ponomarev, J. C. Kim, L. J. Whitman, T. L. Reinecke, and D. Gammon, Engineering electron and hole tunneling with asymmetric InAs quantum dot molecules, Appl. Phys. Lett. **89**, 233110 (2006).

[10] F. Martins, F. K. Malinowski, P. D. Nissen, E. Barnes, S. Fallahi, G. C. Gardner, M. J. Manfra, C. M. Marcus, and F. Kuemmeth, Noise suppression using symmetric exchange gates in spin qubits, Phys. Rev. Lett. **116**, 116801 (2016).

[11] D. Kim, S. G. Carter, A. Greilich, A. S. Bracker, and D. Gammon, Ultrafast optical control of entanglement between two quantum-dot spins, Nat. Phys. **7**, 223 (2011).

[12] H. J. Kimble, The quantum internet, Nature (London) **453**, 1023 (2008).

[13] S. E. Economou, N. Lindner, and T. Rudolph, Optically generated 2-dimensional photonic cluster state from coupled quantum dots, Phys. Rev. Lett. **105**, 093601 (2010).

[14] R. Raussendorf and H. J. Briegel, A one-way quantum computer, Phys. Rev. Lett. **86**, 5188 (2001).

[15] E. Zallo, R. Trotta, V. Kpek, Y. H. Huo, P. Atkinson, F. Ding, T. Ë. Sikola, A. Rastelli, and O. G. Schmidt, Strain-induced active tuning of the coherent tunneling in quantum dot molecules, Phys. Rev. B **89**, 241303(R) (2014).

[16] S. G. Carter, A. S. Bracker, M. K. Yakes, M. K. Zalalutdinov, M. Kim, C. S. Kim, B. Lee, and D. Gammon, Tunable coupling of a double quantum dot spin system to a mechanical resonator, Nano Lett. **19**, 6166 (2019).

[17] G. Burkard, G. Seelig, and D. Loss, Spin interactions and switching in vertically tunnel-coupled quantum dots, Phys. Rev. B **62**, 2581 (2000).

[18] M. Korkusiński and P. Hawrylak, Electronic structure of vertically stacked self-assembled quantum disks, Phys. Rev. B **63**, 195311 (2001).

[19] D. Bellucci, F. Troiani, G. Goldoni, and E. Molinari, Neutral and charged electron-hole complexes in artificial molecules: Quantum transitions induced by the in-plane magnetic field, Phys. Rev. B **70**, 205332 (2004).

[20] D. Jacob, B. Wunsch, and D. Pfannkuche, Charge localization and isospin blockade in vertical double quantum dots, Phys. Rev. B **70**, 081314(R) (2004).

[21] L. G. D. D. Silva, J. M. Villas-BÃ´as, and S. E. Ulloa, Tunneling and optical control in quantum ring molecules, Phys. Rev. B **76**, 155306 (2007).

[22] J. I. Climente, Tuning the tunnel coupling of quantum dot molecules with longitudinal magnetic fields, Appl. Phys. Lett. **93**, 223109 (2008).

[23] J. Planelles, J. I. Climente, F. Rajadell, M. F. Doty, A. S. Bracker, and D. Gammon, Effect of strain and variable mass on the formation of antibonding hole ground states in InAs quantum dot molecules, Phys. Rev. B **82**, 155307 (2010).

[24] J. Phoenix, M. Korkusinski, D. Dalacu, P. J. Poole, P. Zawadzki, S. Studenikin, R. L. Williams, A. S. Sachrajda, and L. Gaudreau, Magnetic tuning of tunnel coupling between InAsP double quantum dots in InP nanowires, Sci. Rep. **12**, 5100 (2022).

[25] H. J. Krenner, M. Sabathil, E. C. Clark, A. Kress, D. Schuh, M. Bichler, G. Abstreiter, and J. J. Finley, Direct observation of controlled coupling in an individual quantum dot molecule, Phys. Rev. Lett. **94**, 057402 (2005).

[26] F. Bopp, J. Rojas, N. Revenga, H. Riedl, F. Sbresny, K. Boos, T. Simmet, A. Ahmadi, D. Gershoni, J. Kasprzak *et al.*, Quantum dot molecule devices with optical control of charge status and electronic control of coupling, Adv. Quantum Technol. **5**, 2200049 (2022).

[27] P. W. Fry, J. J. Finley, L. R. Wilson, A. Lemaître, D. J. Mowbray, M. S. Skolnick, M. Hopkinson, G. Hill, and J. C. Clark, Electric-field-dependent carrier capture and escape in self-assembled InAs/GaAs quantum dots, Appl. Phys. Lett. **77**, 4344 (2000).

[28] See Supplemental Material at http://link.aps.org/supplemental/10.1103/dhjc-fvh3 for further details on the sample structure and theoretical models

[29] M. Bayer, S. N. Walck, T. L. Reinecke, and A. Forchel, Exciton binding energies and diamagnetic shifts in semiconductor quantum wires and quantum dots, Phys. Rev. B **57**, 6584 (1998).

[30] M. Bayer, O. Stern, A. Kuther, and A. Forchel, Spectroscopic study of dark excitons in $In_xGa_{1-x}As$ self-assembled quantum dots by a magnetic-field-induced symmetry breaking, Phys. Rev. B **61**, 7273 (2000).

[31] M. Bayer, G. Ortner, O. Stern, A. Kuther, A. A. Gorbunov, A. Forchel, P. Hawrylak, S. Fafard, K. Hinzer, T. L. Reinecke, S. N. Walck, J. P. Reithmaier, F. Klopf, and F. Schäfer, Fine structure of neutral and charged excitons in self-assembled In(Ga)As/(Al)GaAs quantum dots, Phys. Rev. B **65**, 195315 (2002).

[32] L. Jacak, P. Hawrylak, and A. Wojs, *Quantum Dots* (Springer Science & Business Media, 2013).

[33] Z. Wasilewski, S. Fafard, and J. McCaffrey, Size and shape engineering of vertically stacked self-assembled quantum dots, J. Cryst. Growth **201–202**, 1131 (1999).

[34] R. Colombelli, V. Piazza, A. Badolato, M. Lazzarino, F. Beltram, W. Schoenfeld, and P. Petroff, Conduction-band offset of single InAs monolayers on GaAs, Appl. Phys. Lett. **76**, 1146 (2000).